Ankle springs instead of arc-shaped feet for passive dynamic walkers

Martijn Wisse,
Daan G.E. Hobbelen,
and Remco J.J. Rotteveel
Mechanical Engineering
Delft University of Technology
Delft, The Netherlands
Email: m.wisse@tudelft.nl

Stuart O. Anderson
and Garth J. Zeglin
The Robotics Institute
Carnegie Mellon University
Pittsburgh PA, USA

Abstract— **Passive dynamic walking is interesting for humanoid robots because of the efficient, natural-looking, and naturally stable gait. However, most prototypes so far have been equipped with arc-shaped feet rigidly mounted to the shank, which has been deemed 'non-human', and it prevents certain functions such as standing still. In this paper, we show that the rigid arc feet can be replaced by flat feet that are mounted on ankles with a torsional spring stiffness. The spring stiffness has a similar effect as the foot radius; it reduces the sensitivity to disturbances and thus improves the disturbance handling. We have already implemented the idea in various prototypes, but in this paper we focus on the disturbance behavior of a simple 2D straight-legged passive walking model.**

I. Introduction

Passive dynamic walking has been identified as a promising concept for the development of dynamically walking humanoid robots. The concept was introduced in 1990 by McGeer [10], who showed that a fully unactuated and uncontrolled two-legged mechanism can perform a stable walking motion down a slight incline. The resulting walking motion has a low energetic cost; the floor slope, which represents the amount of energy used per meter traveled per unit of weight, is usually something like 0.01 rad. This is between one and two orders of magnitude smaller [3] than the energetic cost of current state-of-the-art robots [12]. In addition, the walking motion of the passive walkers is generally characterized as natural-looking. Finally, one of the big attractions of the concept is that it leads to simple, affordable, and lightweight robots; in principle they need no sensors, motors, or controls at all.

However, some characteristics of passive dynamic walking have made the concept seem uninteresting for practical robots. One of these characteristics is the need for a downhill slope in the floor. Fortunately, recent research [3] has shown that this slope is not a fundamental property, but rather just a convenient energy source which can be replaced by a variety of other sources. Based on the concept of passive dynamic walking, robots were built that walk on a level floor using ankle push-off [14], [2] or hip actuation [20], [15].

Another alleged drawback of passive dynamic walkers is their use of arc-shaped feet that are rigidly attached to the shank. The arc feet are used because they have a positive effect on the disturbance behavior of the robots, when compared to point feet (i.e. no feet at all). The drawback is that the arc shape does not look human-like. And, perhaps more importantly, the contact with the floor is a point (for 2D models) or a line (for 3D models) which makes the contact conditions more dependent on local floor properties. For 3D models, the friction torque against yaw (rotations around the vertical axis) is often insufficient for the arc foot walkers [4]. Finally, it is not possible to stand still in upright position with arc feet. In summary, a flat foot is expected to not only look more human-like, but also to provide a better friction torque, and to extend the capabilities beyond walking.

The purpose of this paper is to dispel the alleged 'arc foot requirement' for the concept of passive dynamic walking. We show that similarly positive disturbance behavior is obtained with a flat foot that is mounted to an ankle joint with a torsional spring. In the analysis, we restrict ourselves to completely passive models to prevent any confusion with actuation effects (e.g. push-off), which could have additional stability effects.

The publication of this rather elementary study comes after the idea has already successfully been implemented in three different robots, which we present in Section II. Then follows a description of the elementary passive prototype and model in Section III, and a presentation of the results in Sections IV-VI. In Section VII we discuss a possible explanation of the results using the concept of Center of Pressure, followed by the conclusion in Section VIII.

II. Motivation: the idea has already been implemented

Before we conducted the analysis as presented in this paper, we had already implemented the idea in various robots. These robots all have flat feet that are mounted to an ankle joint with a rotational spring stiffness. And these robots all show successful walking motions. However, we did not use these robots to study the ankle spring effect in detail, we only implemented the idea as one of many ideas inside these robots, so we cannot present them as a validation of a theoretical

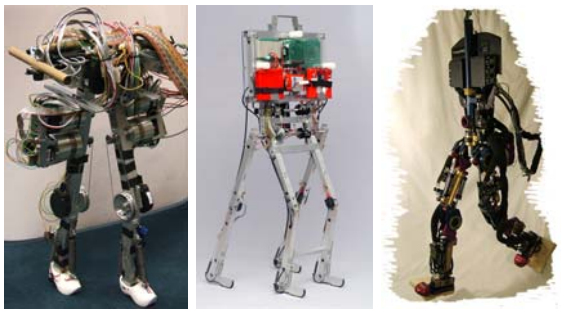

Fig. 1. **(a)** Direct Drive Biped of Carnegie Mellon University. **(b)** Prototype META, the first Delft prototype to walk with flat feet and ankles with springs. **(c)** 3D hydraulic biped built by Sarcos for Carnegie Mellon University.

ankle analysis. Instead, we present the robots here at start of the paper as a motivation for the analysis that follows.

A. CMU Direct Drive Biped

At Carnegie Mellon University, a robot was built with direct drive actuators in the hips and knees (Fig. 1a). Direct drive actuators are basically electric DC motors that have been optimized for torque output, and which are usually applied without any gearbox. The advantage of such actuators for our research is that they add little to no friction and rotational inertia to the joints, unlike conventional drive-train designs with high gear ratios. This biped was built to study powered walking based on passive dynamic principles [1]. The biped walks on a boom so that it essentially possesses 2D dynamics. A previous incarnation of this biped had shown highly successful CPG-controlled ([11], [5]) walking behavior using rigid arc feet. In the current robot, we implemented flat feet mounted on an ankle joint with passive springs instead of rigidly attached arc feet, mainly to see if it could be done. The empirical (anecdotal, i.e. not quantified, yet very certain) result was that it was hardly possible to find successful walking motions when the robot had point feet, while it became almost trivially easy to find stable gait after the feet and springs were mounted. The resultant walking motion has been reported in [1].

B. META

We intend to use the concept of passive dynamic walking as a basis for more versatile and robust humanoid walking robots. By adding ankle joints, it will become possible to implement ankle push-off, an effective way to pump energy into the gait [2]. By using flat feet, we make it possible for the robot to stand upright. Also, this will increase the contact area of the foot, which will be beneficial for future 3D robot designs which often suffer from a lack of friction torque to resist yawing motions [4] (rotation around the vertical axis).

Because of these benefits of flat feet with ankles, we have implemented such feet on our robot META, a minimally actuated biped based on the principles of passive dynamic walking (Fig. 1b). META has two pairs of legs, one inner pair and one outer pair, so that the dynamic behavior is mostly two-dimensional. In addition to the new ankle/foot design, the prototype also uses ankle push-off, swing leg control [16], and it has a bisecting mechanism for the upper body [19], [17].

We first used a simulation study to research which parameters for the ankle and foot design would be optimal for the (pre-existing) robot design [6]. This was mostly a trade-off between energetic cost, robustness (partly determined by ground clearance), and how much time the foot was indeed in full contact with the floor (as opposed to rotating on heel or toe). The resulting parameters were used for the design of the foot and ankle of the prototype. The prototype shows a convincingly stable walking motion (see movies at `www.dbl.tudelft.nl`), which we believe can be partially contributed to the springs in the ankles.

C. CMU/Sarcos Hydraulic Biped

At Carnegie Mellon University, research is in progress on a 3D human scale robot (Fig. 1c) designed and built by Sarcos [www.sarcos.com]. It has seven actuated degrees of freedom in each leg and two in the torso for a total of sixteen degrees of freedom. Each degree of freedom is driven by a linear hydraulic actuator with a flow control servo valve and a force sensor between the actuator and the joint. Each foot is equipped with a six degree of freedom load cell. We have increased the width of the feet in the initial experiments to 0.2 by 0.2m. We placed a material on the corners of the bottom of the feet that absorbs energy at heel strike and has a high coefficient of friction. The size of the robot is 0.77m from hip joint to ankle joint, 0.17 m between the hip joints and 0.39m from hip to knee. The robot weighs approximately 52 kg. The majority of this mass is located in the legs, while the upper body is relatively light. The robot uses a flexible tether to provide hydraulic and electrical power as well as communication to external computers.

The first successful walking experiments with this robot have been reported in [1]. The robot controller was constructed using various ideas from passive dynamic walking. For the ankle joint of the stance foot, we implemented a weak position controller, effectively making the ankle joint behave like a torsional spring. We tuned the spring stiffness and offset just as we did this for the Direct Drive biped, although in that robot it was done in hardware and in this robot in software. Again, we believe that we can partially attribute the successful walking result to the implementation of an spring stiffness in the ankle joint. This believe serves as the motivation for the research in the remainder of this paper.

III. Passive prototype and model

The analysis will be conducted with a model of the prototype shown in Fig. 2. According to the tradition started by McGeer, the prototype has quasi-2D dynamics due to the symmetric construction with an inner pair and an outer pair of legs. With rigid arc feet, the prototype is equal to McGeer's straight-legged walker [10]. The parameters of our incarnation of this prototype are given in Table I. Subsequently, the prototype was equipped with flat feet, ankle joints, and springs, see Fig. 2 and Table I. For both type of feet, the prototype

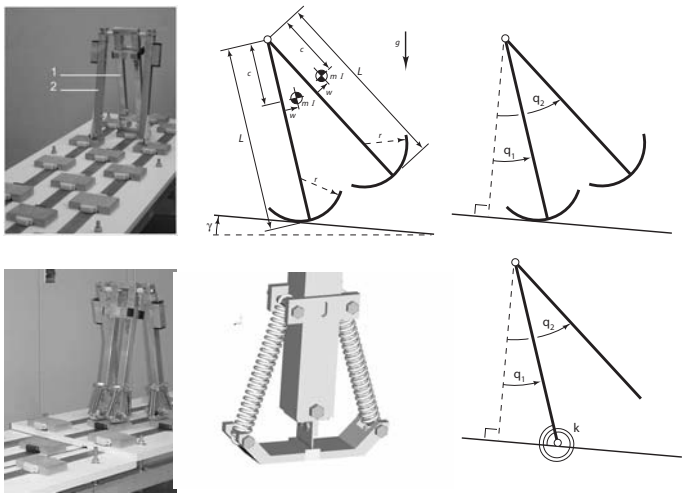

Fig. 2. Passive prototype with arc foot (top) or flat feet mounted on ankles with springs.

has a problem at midstance. Due to the absence of knees, the prototype would always stub its toes when the swing leg passes the stance leg. Therefore, the walking surface is covered with tiles (or 'stepping stones') that have been carefully positioned where the feet are expected to land, see Fig. 2. It takes a few iterations to get this right, and it has to be re-done for every parameter change. It also requires that the person who launches the robot can do so with very repeatable initial conditions.

World			
gravity	g	9.81	$\mathrm{m/s^2}$
slope angle	γ	0.0125	rad
Leg 1 and 2			
length	l	0.4	m
foot radius	r	0 - 0.4	m
CoM location	c	0.1	m
	w	0	m
mass	m	1	kg
moment of inertia	I	0.01	$\mathrm{kgm^2}$
spring stiffness	k	0 - 8	Nm/rad

TABLE I

PARAMETERS FOR A SIMPLE PASSIVE DYNAMIC WALKING MODEL CORRESPONDING TO FIGURE 2. THE GIVEN DEFAULT PARAMETER VALUES WERE CHOSEN TO 1) COMPLY WITH A REALISTIC PROTOTYPE, AND 2) PROVIDE STABLE SIMULATION RESULTS.

The prototype is modeled as a 2D walker with two equal legs, walking down a slight incline. The exact parametrization is given in Fig. 2 and Table I. We assume no rolling resistance, infinite friction (i.e. no slip), and a fully inelastic impact at heel strike, at which the former stance leg immediately loses floor contact. The tiles in the floor, which were necessary for the prototype, do not have to be modeled. Instead, we simply allow the model to let the swing foot pass through the floor around midstance. The derivation of the equations of motion and impact are mostly described in [18].

The model of the ankle joint is slightly simplified. In the prototype, the feet are (light) rigid bodies with their own dynamics. In the model, we ignore their mass. So, in the swing phase, the foot simply doesn't exist, and in the stance phase, we treat it as a part of the floor. The model is therefore a simple point foot model with a torsional spring between the stance leg and the floor.

The behavior of the spring and the foot at heel strike requires special attention. In the prototype, the swing foot lands on the heel. In a short period of time, the spring of that foot is being loaded while the foot rotates around the heel until full, flat contact is reached. While the spring is being loaded, the velocity of the walker decreases, as the kinetic energy is transformed into spring energy. Then, at the instant of full, flat contact, an impact takes place, at which some energy is lost. After this instant, the rear foot starts to unload the spring, putting the spring energy back into the forward motion of the robot. This can be seen as ankle push-off.

We model the above effects in the following way. The simulation of a step is continued until the ankle joint of the swing leg has reached ground level. We calculate how much energy the spring of the front foot needs in this position. Then, instantaneously we decrease the rotational velocity of the rear leg, such that the kinetic energy decrease matches the spring energy increase. Then an impact is calculated in which the rear leg looses support. Subsequently, the rotational velocity of the front leg is instantly increased so that the kinetic energy increase matches the spring energy of the rear foot. In short, we model the foot contact transition as an instantaneous event while respecting the energy transfer between the springs and the forward velocity.

IV. NOMINAL MOTION

The starting point for the analysis is a point foot model with the parameter values of Table I, and with ankle spring stiffness $k = 0$ and foot radius $r = 0$. This model exhibits a stable periodic gait as depicted in Fig. 3. The swing leg (angle q_2) moves from a negative to a positive value following a quasi-sinusoidal motion. The stance leg (angle q_1) moves from a positive to a negative value. Where it crosses the vertical position, the velocity is lower than at the start and the end of the step. The gait is periodic, meaning that the end of the step (after heel strike impact) is identical to the start of the step, and so the motion repeats itself indefinitely. This only occurs for the specific initial conditions shown in Fig. 3 and listed in Table II.

stance leg angle	q_1	0.1671	rad
swing leg angle	q_2	-0.1671	rad
stance leg angular velocity	$\dot{q}_1$	-1.2475	rad
swing leg angular velocity	$\dot{q}_2$	-0.9546	rad

TABLE II

INITIAL CONDITIONS THAT LEAD TO THE PERIODIC GAIT DEPICTED IN FIG. 3 FOR THE MODEL OF FIG. 2 WITH PARAMETER VALUES OF TABLE I AND SPRING STIFFNESS $k = 0$ AND FOOT RADIUS $r = 0$.

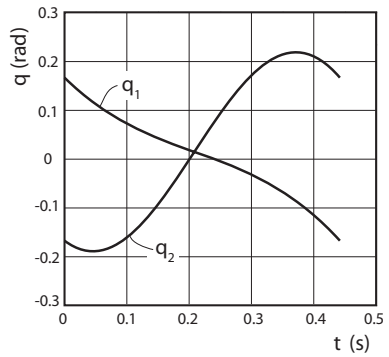

Fig. 3. The walking motion of the simple model with point feet (r=0) and without ankle stiffness (k=0). The stance leg is q_1, the swing leg q_2. This is the motion for a slope of $\gamma = 0.0125$ rad. At steeper slopes, the model makes larger steps (larger initial values for q_1 and q_2), whereas the step frequency remains more or less constant.

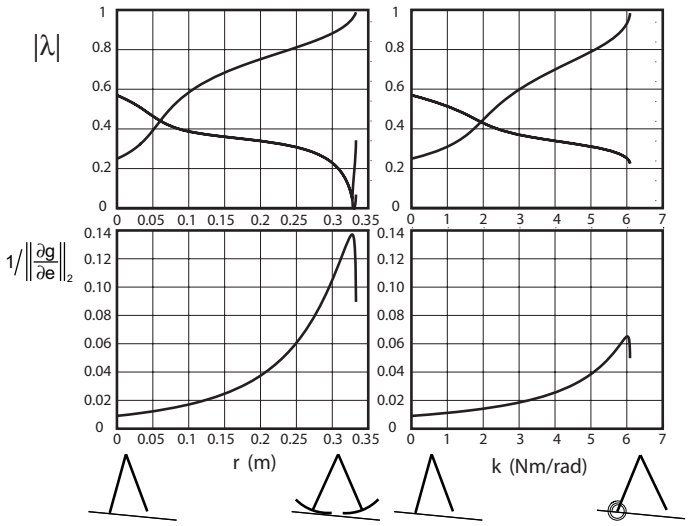

Fig. 4. The effect of an increasing foot radius (left column) and an increasing ankle stiffness (right column).

V. Similar stability and disturbance behavior

This section is the core of this paper. Since all successfully walking prototypes have arc feet with a significant radius, these arc feet must have a positive effect on the disturbance handling. And, since we hypothesize that ankles with springs will have similar dynamic effects, these must have a similarly positive effect on the disturbance handling. We first investigate the effect of foot radius and spring stiffness on the 'Floquet Multipliers', i.e. the standard linearized stability measure for this type of walkers. Because such an analysis does not describe the sensitivity to actual disturbances, we will subsequently research the disturbance rejection capabilities with our new 'Gait Sensitivity Norm'.

A. Floquet Multipliers

Ever since researchers have begun looking at gait as a periodic motion [8], [9], the standard tool for stability analysis has been the study of the 'Floquet multipliers'. These can be seen as 'error multiplication factors' from one step onto the next. They are obtained as follows. First, the periodic gait must be found, so that we have initial conditions for a step that will result in identical initial conditions for the next step. Then, a small perturbation is added to one of the initial conditions, and the resulting deviations for the subsequent step are recorded. By repeating this for each of the initial conditions, we obtain a linear map $\mathbf{A}$ which maps errors from one step onto the next[1]. The eigenvalues of $\mathbf{A}$ are the so-called Floquet Multipliers, indicated with $\boldsymbol{\lambda}$. If the absolute values of *all* Floquet Multipliers are smaller than 1, then all errors will decay step after step, and the gait is stable.

The top row of Fig. 4 shows $|\boldsymbol{\lambda}|$, i.e. the absolute values of the Floquet Multipliers, as a function of foot radius r or ankle spring stiffness k. It appears as if there are two lines in each graph, but there are actually four; the four initial conditions ($\{q_1, q_2, \dot{q}_1, \dot{q}_2\}$) result in a 4x4 matrix $\mathbf{A}$ which has four eigenvalues. However, one of the eigenvalues is always identical to zero by definition, because the initial swing leg angle is always exactly the same (but opposite in sign) as the initial stance leg angle. Or in other words: because the Poincaré Section is defined in state space and not in time. Of the other three Floquet Multipliers, two form a complex conjugate pair, which have the same absolute value. This explains why we see only two lines in the graphs. Only for $r \approx 0.33$ m one can identify three different Floquet Multipliers in the graph.

Figure 4 shows that the arc foot model is stable up to an arc radius of $r = 0.333$ m, which is close to the leg length $l = 0.4$ m. The ankle model is stable up to a spring stiffness of $k = 6.09$ Nm/rad. Above these values, we could not find normal periodic walking motions. The development of the Floquet Multipliers is very similar for the two models, which indicates similarity in the way that disturbances are handled.

B. Gait Sensitivity Norm

Floquet Multipliers only have limited value, because they describe the *linearized* step-to-step behavior without considering the sensitivity to actual disturbances. Although they make a clear distinction between *stable* ($\max|\boldsymbol{\lambda}| < 1$) and *unstable* ($\max|\boldsymbol{\lambda}| > 1$), there is no further correlation between $\boldsymbol{\lambda}$ and the maximally allowable disturbances [13].

In order to investigate the sensitivity to disturbances, we introduced the Gait Sensitivity Norm [7], $\|\frac{\partial \mathbf{g}}{\partial \mathbf{e}}\|_2$. Although this is also a linearized quantity, we have shown [7] that it has a strong correlation with the maximally allowable disturbance; the lower this sensitivity value, the larger of a disturbance the robot can handle. Therefore, in Fig. 4 we present the inverse of the sensitivity norm, $1/\|\frac{\partial \mathbf{g}}{\partial \mathbf{e}}\|_2$. A high value here means that large disturbances can be handled.

For the calculation of the Gait Sensitivity Norm, one has to choose the type(s) of disturbances $\mathbf{e}$ of interest. We argue

[1]The full nonlinear map is called a Poincaré Map. The heel strike event, which we chose as the telltale event at which we want to compare the states, is called the Poincaré Section. The linear map $\mathbf{A}$ is also called a Monodromy matrix.

that a single step-down (or up) in the floor is a representative disturbance for most walking devices.

With a simulation of a single step after the disturbance, we know how this disturbance influences the initial conditions $\mathbf{v} = \{q_1, q_2, \dot{q}_1, \dot{q}_2\}$ for the next step. The (linear) transfer matrix is

$$\mathbf{B} = \frac{\partial \mathbf{v}}{\partial e} \tag{1}$$

Then, with the linear error map $\mathbf{A}$ that we presented earlier, we know how errors on the initial conditions $\mathbf{v}$ are propagated step after step.

Finally, we need to decide what characteristic measurement $\mathbf{g}$ in the gait will accurately indicate how likely it is that the robot will fall. A thorough study in [7] has shown that for a 2D passive walking model like ours, the variability of the step time, ΔT, is very indicative of an upcoming fall. The reason is that the passive swing leg requires some time to reach a forward position, and if this time is not available the robot will fall forward. If small disturbances $\mathbf{e}$ cause large variations in step time ΔT, then it is highly likely that the real robot will fall forward. The linear map from variations in the initial conditions $\mathbf{v}$ to variations of step time ΔT is obtained through simulation again[2]:

$$C = \frac{\partial T}{\partial \mathbf{v}} \tag{2}$$

All transfer matrices together (including a direct effect D which maps disturbances $\mathbf{e}$ directly to variations of the step time ΔT) give the block diagram of Fig. 5. We then take the H_2 norm of the complete block diagram. In essence, this means that we take the sum of the squares of the step time variations of all subsequent steps after a single disturbance, until the effect has died out. In short:

$$GaitSensitivityNorm = \|\frac{\partial T}{\partial e}\|_2 = \frac{1}{e}\sqrt{\Delta T_1^2 + \Delta T_2^2 + ...} \tag{3}$$

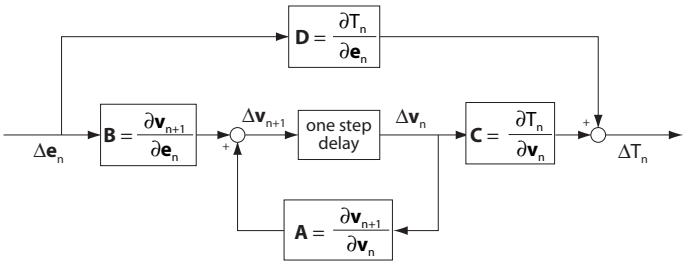

Fig. 5. Sensitivity matrices determine how an external disturbance (a step-down in the floor) is transmitted to the initial conditions of the next step (**B**), how errors in these initial conditions propagate step after step (**A**), and how these errors are transmitted to variations in the step time (**C**). There is also a direct effect from the step-down disturbance to the step time of that same step (**D**).

The bottom row of Fig. 4 shows the effect of foot radius r or ankle stiffness k on the gait sensitivity norm $\|\frac{\partial T}{\partial \mathbf{e}}\|_2$. We plot the inverse, $1/\|\frac{\partial T}{\partial \mathbf{e}}\|_2$ for easy interpretation; a higher value here means better disturbance handling.

The main conclusion from Fig. 4 is that both parameters have the same effect: the larger r (for the rigid arc foot model) or k (for the model with flat feet on ankles with springs), the better the disturbance behavior. The similarity here shows that both r and k have a similarly positive effect on the disturbance behavior.

Note that it would not be wise to use a very large radius (or spring stiffness) in a real prototype, because the system gets close to instability (top row of Fig. 4). The Gait Sensitivity Norm predicts good disturbance behavior but a small parameter error may destabilize the system. Also, the feet will have to be so large that tripping becomes more of a problem. In practice, we usually apply a radius of approximately 1/3 to 1/2 of the leg length.

VI. Not quite similar gait

The spring stiffness k and the foot radius r have a similar effect on the disturbance behavior. Now, we investigate how similar or dissimilar their effect is on the walking motion. Fig. 6 shows how the initial conditions vary as a function of r or k. The top graphs display the initial stance leg angle q_1. The initial swing leg angle q_2 is not shown, because by definition it is always the same (but opposite in sign) as q_1. The graph shows that the robot will take larger steps when it has a larger foot radius r or a larger spring stiffness k. The effect of both parameters is similar, but it is much more pronounced for the arc foot model.

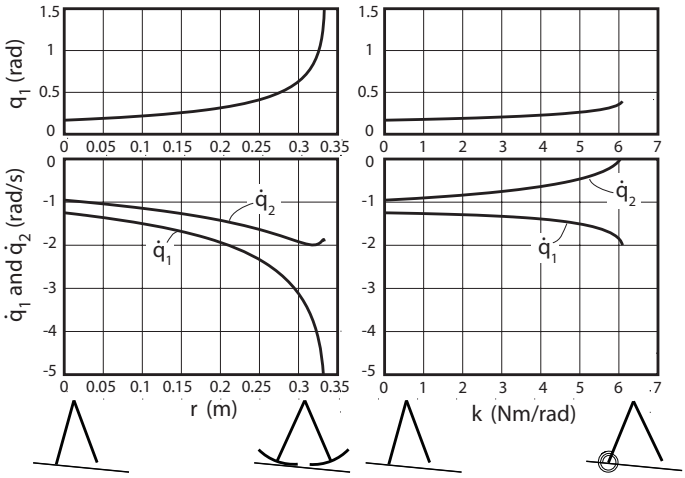

Fig. 6. The effect of an increasing foot radius (left column) and an increasing ankle stiffness (right column).

The bottom graphs of Fig. 6 show the variation of the initial velocities $\{\dot{q}_1, \dot{q}_2\}$. The stance leg velocity $\dot{q}_1$ increases for both parameters. Thus, for a larger r as well as for a larger k, both the step length and the forward velocity increase. However, the effect of the parameters on the initial swing leg velocity $\dot{q}_2$ is not quite similar. This means that the swing leg will make a different motion. This difference is caused by a

[2]these results can be recorded simultaneously with the simulations for obtaining matrix **A**, so no extra calculation time is required.

difference in the foot support transition behavior. Since we have a simplified model for the transitions of the spring ankle model, we are not completely sure how much of the difference in initial conditions can be attributed to that simplification. We believe that this difference is not significant, but further research is recommended.

VII. Explanation

We have demonstrated that larger r and k result in better disturbance behavior. Now we have to try and explain these results. Unfortunately, any attempt to catch the behavior of a complex hybrid dynamical system in simple explanations will unavoidably lead to oversimplification. Nevertheless, we feel that it is worthwhile to mention the 'two main effects' of r and k on the disturbance behavior.

First, by changing r and k, we change how the step-down e affects the initial conditions $\mathbf{v} = \{q_1, q_2, \dot{q}_1, \dot{q}_2\}$. This effect is captured with the matrix **B**, Eq. (1). The graphs in the top row of Fig. 7 show four lines, one for each element in B. Each line represents the sensitivity of one of the initial conditions to a step-down disturbance e. Some of the sensitivities decrease and some don't, one cannot draw concrete conclusions from this. There is a significant difference between the effect of r and k. We suspect that this difference is related to difference in how the step length increases (see q_1 in Fig. 6), which is much more pronounced for r than for k. For future research we recommend to perform a comparative study where the step length is kept constant by adjusting the slope angle γ.

Second, both r and k decrease the effect of variations in the initial conditions $\mathbf{v}$ on the variations of the step time ΔT. This effect is captured with the matrix **C**, Eq. (2). The graphs in the bottom row of Fig. 7 show four lines, one for each element in C. Each line represents how the step time T varies as a function of errors on one of the initial conditions $\{q_1, q_2, \dot{q}_1, \dot{q}_2\}$. Clearly, both k and r have a positive effect; both parameters make the step time less sensitive for errors on the initial conditions.

We hypothesize that this effect is mainly due to the forward progression of the Center of Pressure. In order to explain this, we first have to consider the stance leg as a static (unstable) inverted pendulum, standing still in upright position. At $r = 0$ and $k = 0$, the instability is 'worst' meaning that any deviation from the upright position will increase quickly. After one step time T (approx. 0.5 s, see Fig. 3), any deviation will have increased by a factor of 15. Now, for the stance leg in motion, the same is approximately true. So, any error on the initial conditions in Fig. 3 will lead to a 15-fold error by the time of heel strike. This means that small errors in $\{q_1, q_2, \dot{q}_1, \dot{q}_2\}$ lead to large variations in any output variable, such as step time T. Now, the effect of a foot radius r is a decrease of the error multiplication factor. For example, if r equals the inverted pendulum length, then the stance leg would roll forward with a constant velocity. The Center of Pressure (CoP), which is the same as the contact point, travels forward exactly as much as the Center of Mass (CoM). Any error in the initial conditions would just stay there, i.e. it increases by a factor 1. Thus, small

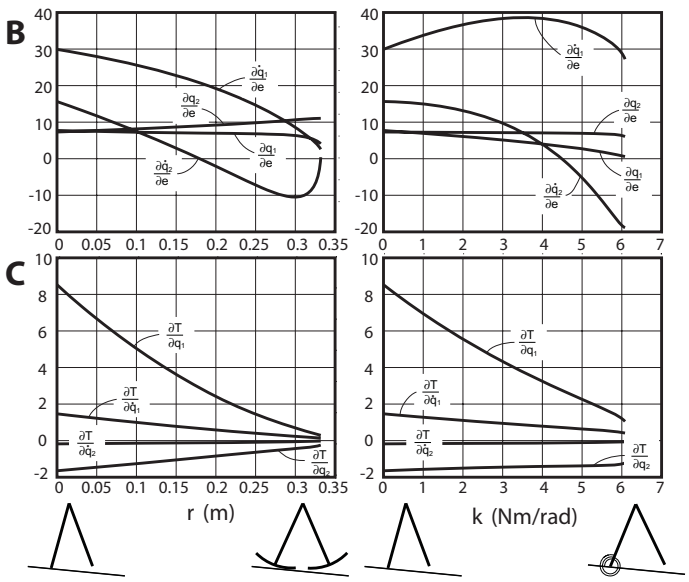

Fig. 7. The effect of an increasing foot radius (left column) and an increasing ankle stiffness (right column) on the transfer matrices **B** and **C**. The decreasing trend of the sensitivities indicates a smaller sensitivity (and thus a better resistance) to disturbances.

errors in $\{q_1, q_2, \dot{q}_1, \dot{q}_2\}$ only lead to small variations in T. The ankle spring has the exact same effect. And one can identify a similar forward travel of the CoP. The CoP is a function of the spring stiffness k, the stance leg angle q_1 and the vertical contact force which is approximately the weight of the robot $2mg$ (there are two legs each with mass m). If we want this CoP to be the same function of q_1 as it is for the arc foot model, we get the following equations:

$$\left.\begin{array}{rcl} d_{arc} & = & q_1 r \\ d_{spring} & = & q_1 k/(2mg) \end{array}\right\} \rightarrow k = 2mgr \qquad (4)$$

where the amount of forward travel of the CoP is d_{arc} for the arc foot model and d_{spring} for the ankle model. For our parameter values of leg mass $m = 1$ and gravity $g = 9.81$, we obtain the following relationship for equivalent CoP behavior:

$$k = 19.62r \qquad (5)$$

And indeed, if one inspects the graphs in Figs. 4, 6, and 7, we find approximately corresponding behavior according to the equivalence in Eq. 5. Thus, we conclude that flat feet with ankles and springs not only have a similar effect as rigid arc feet, but that we can even calculate an equivalent ankle stiffness using equation (4).

VIII. Conclusion and Recommendations

The rigid arc feet, well known from passive dynamic walking literature, can equally well be replaced by flat feet mounted on ankles with a torsional spring. The arc radius has a positive effect on the disturbance behavior, and the spring stiffness has a similar effect. In order to find an equivalent stiffness to replace a certain arc radius, one must match the forward progression of the center of pressure.

Our main recommendation is to use flat feet mounted on ankles with springs for all future passive or semi-passive walking robots. We also recommend that the research presented here is validated with a more accurate model of the heel strike transition.

ACKNOWLEDGEMENTS

Thanks to Arend Schwab for modeling suggestions. M Wisse was supported by the Dutch Technology Fund STW and by the NWO, the Netherlands Organization for Scientific Research. This material is also based upon work supported in part by the National Science Foundation under NSF Grants CNS-0224419, DGE-0333420, and ECS-0325383.

REFERENCES

[1] S. O. Anderson, M. Wisse, C. G. Atkeson, J. K. Hodgins, G. J. Zeglin, and B. Moyer. Powered bipeds based on passive dynamic principles. In *Proc. of IEEE/RAS International Conference on Humanoid Robots*, pages 110–116, Tsukuba, Japan, 2005.

[2] S. H. Collins and A. Ruina. A bipedal walking robot with efficient and human-like gait. In *Proc., IEEE Int. Conf. on Robotics and Automation*, Barcelona, Spain, 2005. IEEE.

[3] S. H. Collins, A. Ruina, R. L. Tedrake, and M. Wisse. Efficienct bipedal robots based on passive-dynamic walkers. *Science*, 307:1082–1085, February 18 2005.

[4] S. H. Collins, M. Wisse, and A. Ruina. A two legged kneed passive dynamic walking robot. *Int. J. of Robotics Research*, 20(7):607–615, July 2001.

[5] G. Endo, J. Morimoto, J. Nakanishi, and G. Cheng. An empirical exploration of a neural oscillator for biped locomotion control. In *Proc., IEEE Int. Conf. on Robotics and Automation*, volume 3, pages 3036 – 3042. IEEE, 2004.

[6] D. G. E. Hobbelen and M. Wisse. Ankle joints and flat feet in dynamic walking. In *Proc., Int. Conf. on Climbing and Walking Robots*, Madrid, Spain, 2004. CLAWAR.

[7] D. G. E. Hobbelen and M. Wisse. A disturbance rejection measure for limit cycle walkers: the gait sensitivity norm. Submitted to IEEE Transactions on Robotics, 2006.

[8] Y. Hurmuzlu and G. D. Moskowitz. Bipedal locomotion stabilized by impact and switching: I. two and three dimensional, three elements models, ii. structural stabilityanaly sis of a four element bipedal locomotion model. *Dynamics and Stability of Systems*, 2(2):73112, 1987.

[9] T. McGeer. Powered flight, child's play, silly wheels, and walking machines. In *Proc., IEEE Int. Conf. on Robotics and Automation*, pages 1592–1597, Piscataway, NJ, 1989.

[10] T. McGeer. Passive dynamic walking. *Int. J. Robot. Res.*, 9(2):62–82, April 1990.

[11] J. Morimoto, G. J. Zeglin, and C. G. Atkeson. Minimax differential dynamic programming: application to a biped walking robot. In *Proc., Int. Conf. on Intelligent Robots and Systems*, volume 2, pages 1927 – 1932. IEEE, 2003.

[12] Y. Sakagami, R. Watanabe, C. Aoyama, S. Matsunaga, N. Higaki, and M. Fujita. The intelligent asimo: System overview and integration. In *Proc., Int. Conf. on Intelligent Robots and Systems*, pages 2478–2483, Lausanne, Switzerland, 30 September - 4 October 2002.

[13] A. L. Schwab and M. Wisse. Basin of attraction of the simplest walking model. In *Proc., ASME Design Engineering Technical Conferences*, Pittsburgh, Pennsylvania, 2001. ASME. Paper number DETC2001/VIB-21363.

[14] R. Tedrake, T.W. Zhang, M.-F. Fong, and H.S. Seung. Actuating a simple 3D passive dynamic walker. In *Proc., IEEE Int. Conf. on Robotics and Automation*, 2004.

[15] M. Wisse. Three additions to passive dynamic walking: actuation, an upper body, and 3d stability. *Int. J. of Humanoid Robotics*, 2(4):459–478, December 2005.

[16] M. Wisse, C. G. Atkeson, and D. K. Kloimwieder. Swing leg retraction helps biped walking stability. In *Proc. of IEEE/RAS International Conference on Humanoid Robots*, pages 295–300, Tsukuba, Japan, 2005.

[17] M. Wisse, D. G. E. Hobbelen, and A. L. Schwab. Adding the upper body to passive dynamic walking robots by means of a bisecting hip mechanism. Submitted to *IEEE Trans. on Robotics*, 2004.

[18] M. Wisse and A. L. Schwab. First steps in passive dynamic walking. In *Proc., Int. Conf. on Climbing and Walking Robots*, Madrid, Spain, 2004. CLAWAR.

[19] M. Wisse, A. L. Schwab, and F. C. T. van der Helm. Passive dynamic walking model with upper body. *Robotica*, 22:681–688, 2004.

[20] M. Wisse and J. van Frankenhuyzen. Design and construction of Mike; a 2D autonomous biped based on passive dynamic walking. In H. Kimura and K. Tsuchiya, editors, *Adaptive Motion of Animals and Machines*, pages 143–154, Tokyo, 2006. Springer–Verlag.